J Solid State Electrochem (2018) 22:41–49
DOI 10.1007/s10008-017-3719-8

ORIGINAL PAPER

Novel potential type electrochemical chiral recognition biosensor for amino acid

Yanyang Guo[1] · Runrun Yao[1] · Zimeng Wang[1] · Yufan Zhang[1] · Mengjing Cui[1] · Qiuyue Zhao[1] · Huan Wang[1]

Received: 24 March 2017 / Revised: 27 July 2017 / Accepted: 30 July 2017 / Published online: 7 August 2017

Abstract Novel potential type electrochemical chiral biosensing system with unique capability of distinguishing and quantitating of tyrosine (Tyr) enantiomers by L-cysteic acid and left-handed chiral carbonaceous nanotubes (L-CCNT) modified glassy carbon electrode (L-Cys/L-CCNT/GCE) was first developed. The effect of sweep cycles of L-Cys and the kinds of L-CCNT on electrochemical chiral biosensing performance of L-Cys/L-CCNT/GCE were investigated. The electrochemical identification and quantitative determination of L- and D-tyrosine in their mixed solution were successfully achieved based on the different oxidation potential signals. The chiral structure of L-CCNT, the aromatic ring of Tyr, and also the intermolecular hydrogen bond between cysteic acid (CyA) and Tyr could possibly produce the difference in the free energy, which reflects as potential difference of L- and D-tyrosine. A good linear relationship between the potential, current, and different concentration ratios of L- and D-Tyr was obtained. Our present work realizes the simultaneous detection of Tyr enantiomers in their mixed solution based on the different potential signals, and it is of far-reaching significance in real electrochemical chiral biosensor study.

Keywords Electrochemical chiral biosensing · Potential type · Left-handed chiral carbon nanotube · Tyrosine enantiomers

✉ Yufan Zhang
hyxq.401@163.com

✉ Huan Wang
zwhsjzl@163.com

[1] Key Laboratory of Analytical Science and Technology of Hebei Province, College of Chemistry and Environmental Science, Key Laboratory of Medicinal Chemistry and Molecular Diagnosis, Ministry of Education, Hebei University, 071002 Baoding, People's Republic of China

Introduction

Chirality is a determinative property of most biological molecules; the stereoselectivity of chemical and biochemical processes often depends on recognizing and discriminating one of the chiral enantiomers [1, 2]. Thus, the chiral recognition of enantiomers is very essential in chemical and biological science.

Although high-performance liquid chromatography, capillary electrochromatography, and other methods have been widely employed to discriminate enantiomers [3–6], the weaknesses such as high cost and time-consuming have not been overcome [7]. Electrochemical method provides a simple and rapid chiral analysis technique. The chiral recognition can be evaluated through the changes of electrochemical signals in the presence of the probe molecules [8, 9]. Research of amino acid isomers using electrochemical method has attracted wide interests. Some important works has been reported for electrochemical recognition of tryptophan isomers and showed satisfactory results [10–14]. Therefore, developing a new electrochemical chiral biosening system for more amino acid becomes an important research area.

Tyrosine (Tyr) plays an important role in regulating various biological signaling molecules such as epinephrine, norepinephrine, and dopamine, which are related to mood. Due to the importance of Tyr, monitoring it in food and pharmaceutical industries as well as in clinical diagnosis becomes significant. On the other hand, the investigation of chiral amino acids remains fundamentally significant in exploring the origin of life [4], but currently, there are still barriers for discrimination due to their similar physical and chemical properties [15].

Great efforts have been made to recognize Tyr enantiomers. Liang et al. fabricated electrochemical sensors based

on nickel electrode by molecularly imprinting D/L-Tyr on polypyrrole films to form complementary cavities for subsequent template recognition [7]. Wang et al. introduced an electrochemical sensor based on bovine serum albumin enantioselective films coupled with silver-enhanced gold nanoparticles [16]. These works are mainly focused on the different peak current signal between enantiomer in the solution containing only L- or D-amino acid. Actually, L- and D-amino acid usually coexist in the mixture, and their detection based on peak current is not the real separation and detection of enantiomers. These limitations would possibly influence the further application of chiral electrochemical sensors. Up to now, the electrochemical chiral biosensor employing peak potential as electrochemical signal has been rarely reported. Moreover, as far as we are aware, there is few attention given to the study of electrochemical chiral biosensor with enantiopure chiral carbon nanotubes (100% L type or 100% R type chiral carbon nanotubes) as recognition interface.

Selective synthesis of enantiopure chiral carbon-based nanotubes (CNTs) is still a formidable challenge that remains unsolved. Most of the CNTs that are grown by chemical vapor deposition are mixtures of equal amounts of left- and right-handed helical structures, which do not have optical activity [17, 18]. To obtain enantiopure chiral CNTs, it is essential to enrich and separate racemic mixtures through so-called enantioenrichment.

In the present work, left-handed chiral carbonaceous nanotubes (L-CCNT) are prepared by the one-step carbonization of self-assembled chiral polypyrrole (CPPy) nanotubes. The CPPy nanotubes are templated by self-assembly of left chiral amphiphilic glutamic acid molecules and subsequent polymerization of the pyrroles. The obtained L-CCNT is 100% left-handed double-helical morphology and used as the chiral recognition interface. For the first time, we build a chiral interface employing L-cysteine (L-Cys) and left-handed chiral carbon nanotube (L-CCNT) to identify the potential differences of the two enantiomers. Moreover, we plan to use the potential difference signal to realize quantitative detection of different concentration ratios of Tyr enantiomers in their racemic mixture. This work provides a simple, effective, and economic way to quantitatively analyze Tyr enantiomers in racemic mixture, as well as offers a novel route for the constructing of electrochemical chiral biosensor.

Experimental

Reagents and apparatus

L-Cys, L-glutamic acid, L-Tyr, D-Tyr, myristoyl chloride, and pyrrole were purchased from Aladdin Industrial Corporation (shanghai, China). All other reagents were of analytical grade and used as received without further purification. Double-distilled water was used throughout the whole experiment. The 0.1 M phosphate buffer solution (PBS, pH 7.4) prepared from Na_2HPO_4, NaH_2PO_4, and H_3PO_4 was employed as supporting electrolyte.

Electrochemical detection was performed on a Autolab electrochemistry workstation (PGSTAT-302N, Switzerland metrohm) with a conventional three-electrode system. A platinum electrode was used as the counter electrode, and the reference electrode was an Ag/AgCl electrode. The working electrode was a glassy carbon electrode (GCE) modified with L-CCNT (L-CCNT/GCE).

The transmission electron microscopy (TEM) images were recorded on a JEM-2100F transmission electron microscope (JEOL, Japan) operating at 200 kV. Scanning electron microscopy (SEM) images were determined with a Philips XL-30 ESEM operating at 3.0 kV. X-ray photoelectron spectra (XPS) was collected using an ESCALAB-MKII 250 photoelectron spectrometer (VG Co.) with Al-Ka X-ray radiation as the X-ray source for excitation.

Preparation of L-CCNT-X samples

Amino acid surfactant C_{18}-L-Glu was first prepared according to the following step [19]: 35.5 g of L-glutamic acid was dissolved in a mixed solution of deionized water (140 mL), acetone (120 mL), and NaOH (19.2 g). The obtained solution was stirred vigorously under 30 °C; then, 60.5 g of myristoyl chloride was added into the mixed solution drop by drop under ice-cooling condition and 20 mL of NaOH (0.2 M) was added to keep the pH 12 simultaneously. The reaction mixture was stirred for additional 1 h and acidified to pH 1 with HCl. Finally, the surfactant C_{18}-L-Glu was obtained by washing the sample with deionized water and petroleum ether, and then freeze-drying under − 60 °C.

The enantiopure L-CCNT-X sample was prepared by a one-step carbonization of self-assembled chiral polypyrrole nanotubes according to the method reported by Liu et al. [20]. In a typical procedure, C_{18}-L-Glu (0.06 mmol) was dissolved in methanol (12.9 mL); then, pyrrole (2.4 mmol) and deionized water (60 mL) were added and stirred for 10 min. A total of 2.0 M of precooled ammonium persulfate aqueous solution was added into the mixture and stirred for another 30 min. The chiral polypyrrole nanotube was obtained by filtration, washing and then drying at 40 °C in vacuum. Finally, the enantiopure L-CCNT-X sample was obtained by carbonizing chiral polypyrrole nanotube at different temperatures for 6 h under an Ar atmosphere. The different L-CCNT-X samples carbonized at 500, 700, and 900 °C were denoted as L-CCNT-1, L-CCNT-2, and L-CCNT-3, respectively.

Preparation of the modified electrode

GCE was polished before each experiment with 0.05 μm alumina powder and rinsed thoroughly with doubly distilled water. Then, the cleaned electrode was dried with high-purify nitrogen for the next modification. To prepare the modified electrode, 1 mg of the as-prepared L-CCNT-X sample was dispersed in 1 mL of dimethyl formamide (DMF); a homogeneous suspension (1 mg/mL) was obtained upon bath sonication. The L-CCNT-X/GCE was prepared by casting 5 μL of the L-CCNT-X suspension on the surface of GCE, and the solvent was dried under an infrared lamp. The L-CCNT-X/GCE was first scanned to steady by cyclic voltammetry (CV) from 0.40 to 0.90 V for 10 cycles at the scan rate of 50 mV/s in 0.1 M PBS (pH 7); then, the L-CCNT-X/GCE was scanned again from − 0.60 to 2.0 V for 15 cycles at the rate of 100 mV s^{-1} in PBS (pH 7.4) containing 0.01 M L-Cys; the L-Cys/L-CCNT/GCE was obtained. Finally, the L-Cys/L-CCNT/GCE was rinsed with double-distilled water for removing the residues. L-Cys/GCE was prepared by using the same method on the bare GCE. The construction of electrochemical chiral electrode interface and the chiral biosensing mechanism for L-Tyr and D-Tyr are shown in Fig. 1.

Results and discussion

Characterization of L-CCNT-X

The electrocatalytic activity of carbon nano-materials greatly depends on their morphology and microstructure. In this paper, SEM and TEM were employed to research the morphology of L-CCNT-X. Figure 2a–d shows the SEM images of the three kinds of left-handed CCNTs synthesized at different carbonization temperatures (donated as L-CCNT-1, L-CCNT-2, and L-CCNT-3, respectively). As can be observed, the three CCNTs are typically composed of left-handed double-helical chiral nanotubes with the same morphology. Moreover, the double-helical morphology of the L-CCNT is kept well at 900 °C, as indicated by black arrows in Fig. 2d. Figure 2e shows the high-resolution SEM image of L-CCNT-3; the double-helical morphology can be clearly seen, which further indicates the stability of the double-helical morphology. Furthermore, the diameters of the three kinds of nanotubes are in the range of 40–73 nm, the outer diameter of the L-CCNTs reduces slightly, and the surface of the L-CCNT becomes folded as the carbonization temperature increases. The TEM images in Fig. 2f, g further suggest that the L-CCNT-3 possess double-helical structure with inner tubes. Additionally, L-CCNTs carbonized at high temperature (900 °C) shows a layered arrangement with a rough surface, which may be the characteristic structure of graphitized carbon. These structural characteristics are beneficial to accelerate the processes of mass transfer and electron transfer.

To further explore the compositions and chemical configurations of the L-CCNT-X samples, X-ray photoelectron spectra were recorded (XPS, Fig. 3a–c). The XPS spectra shows different binding energies, attributing to C1s, N1s, and O1s (insert of Fig. 3a–c). The nitrogen element originates from the polypyrrol molecule and amino acid surfactant C_{18}-L-Glu. From the data of XPS, the atomic contents of C, N, and O are 81.68, 5.3, and 13.02 in L-CCNT-1; 84.3, 4.0, and 11.7 in L-CCNT-2; and 79.33, 1.58, and 19.09 in L-

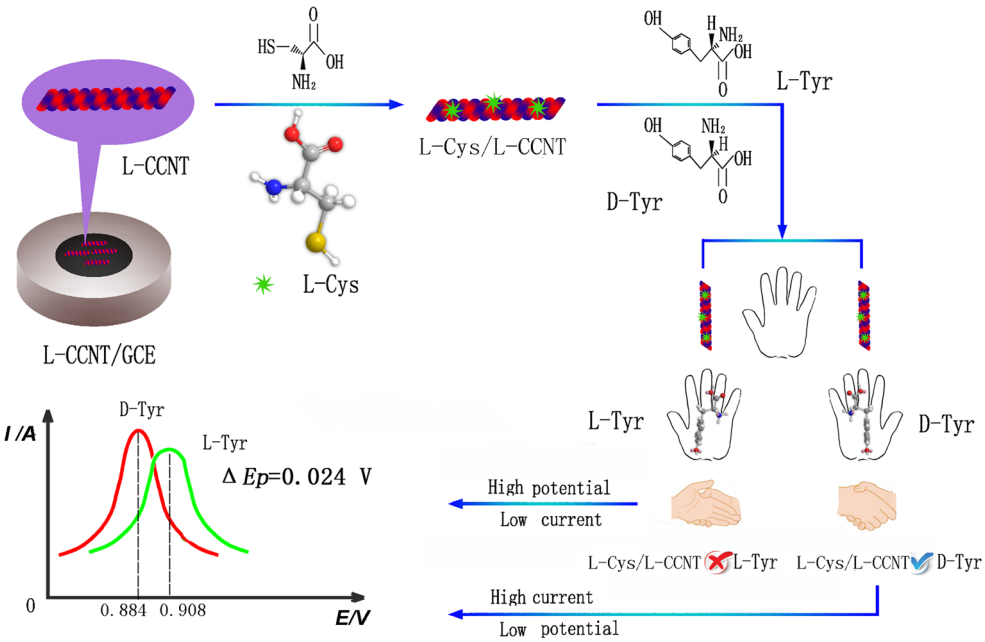

Fig. 1 Illustration of construction of chiral electrode interface and the chiral biosensing mechanism for L-Tyr and D-Tyr

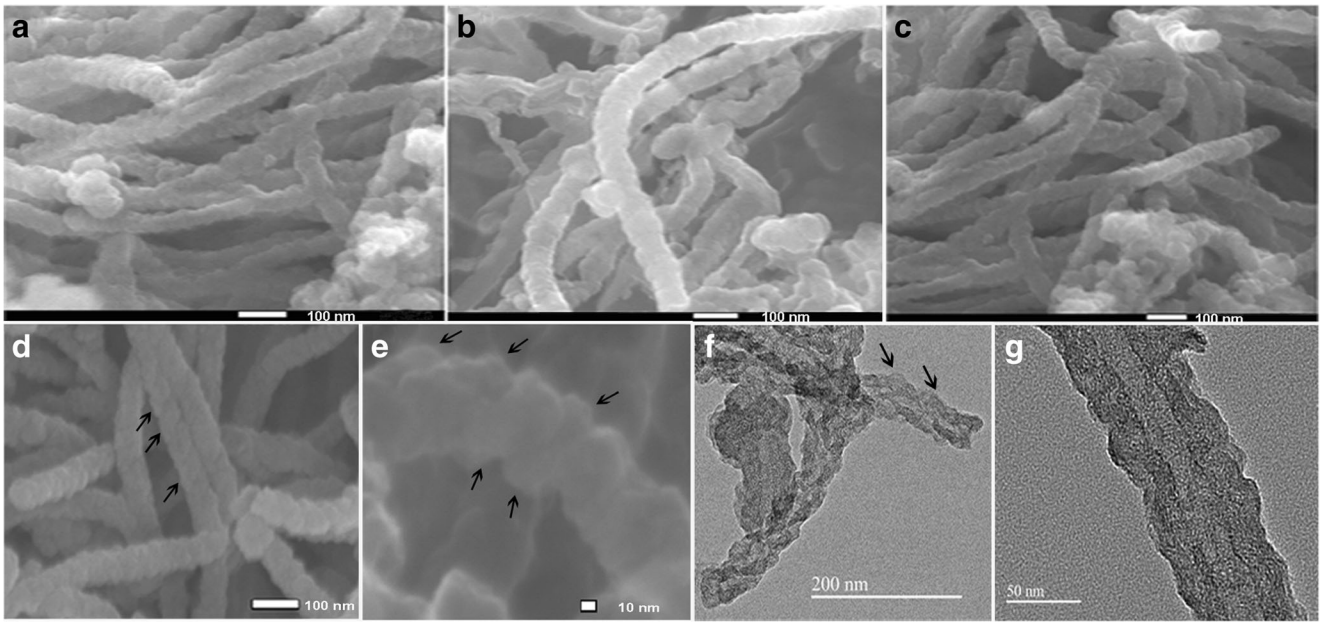

Fig. 2 SEM images of **a** L-CCNT-1, **b** L-CCNT-2, and **c**, **d** L-CCNT-3. **e** High-resolution SEM image of L-CCNT-3. **f** TEM image of L-CCNT-3. **g** High-resolution TEM (HRTEM) image of L-CCNT-3

CCNT-3, respectively. With the increase of pyrolysis temperature, the overall nitrogen content decreases [21] and oxygen content increases in different L-CCNT samples. High-resolution N1s XPS spectra (Fig. 3a–c) can be deconvoluted into three different signals with binding energies of 398.0, 400.0, and 401.3 eV that correspond to pyridinic N, pyrrolic N, and graphitic N, respectively. Moreover, the three peaks significantly change with the pyrolysis temperature, which indicates that different N-bonding congurations have different stability. With the increase of pyrolysis temperature, both the pyridinic N and pyrrolic N are largely decreased, implying that these species are less stable at high temperatures.

Circular dichroism (CD) is the measure method for differential absorption of left- and right-handed circularly polarized light. As can be seen from the Fig. 3d, the L-CCNT-3

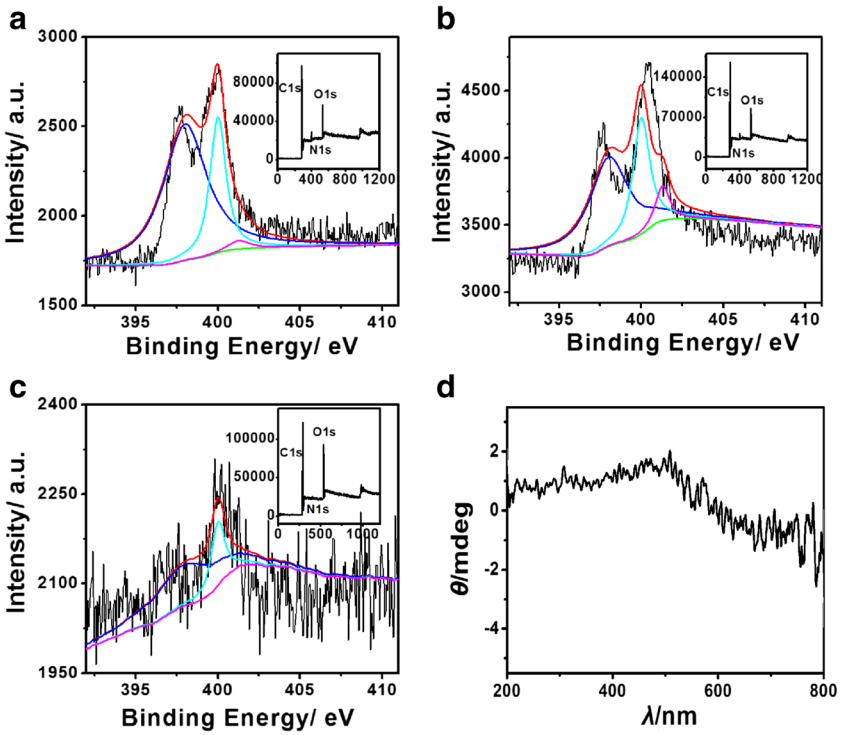

Fig. 3 High-resolution N1s XPS spectra of **a** L-CCNT-1, **b** L-CCNT-2, and **c** L-CCNT-3, insert: XPS spectra. **d** CD spectra of L-CCNT-3

sample shows a single CD signal in the corresponding absorption region, which indicates the enantiopure left-handed chiral structure of our prepared carbonaceous nanotubes.

Chiral selective recognition and detection of Tyr enantiomers on different electrodes

The CVs of L-Cys depositing on GCE are shown in Fig. 4a. It can be clearly seen that two peaks appear at the potential of 0.60 and 1.47 V, which come from the oxidation of L-Cys to L-cystine [22, 23] and chemisorbing molecules (cysteic acid (CyA)) [24]. CyA is the end product of Cys oxidation and can be strongly adsorbed at electrode [25]. This indicates that L-Cys has been electrodeposited on L-CCNT-X successfully. Figure 4b shows the DPVs of 0.75 mM L-Tyr or D-Tyr on bare GCE. The E_p of L-Tyr and D-Tyr on bare GCE is observed at 0.930 V (curve a) and 0.922 V (curve b). Figure 4c shows the DPVs of 0.75 mM L-Tyr or D-Tyr on L-Cys/GCE; the E_p of L-Tyr and D-Tyr are located at 0.892 V (curve c) and 0.880 V (curve d). The difference of peak potential (ΔE_p) is 12 mV. The increased ΔE_p indicates that L-Cys can recognize L-Tyr and D-Tyr, and it has different interreactions with the enantiomer. Inset of Fig. 4d shows the DPVs of L-Tyr and D-Tyr on L-CCNT-3/GCE; the ΔE_p is 16 mV of L-Tyr and D-Tyr, larger than that on GCE and L-Cys/GCE. The result indicates that L-CCNT-3 with unique L type chiral helical structure may have different spatial interaction with L-Tyr and D-Tyr; the difference of L-CCNT-3 and L/D-Tyr attachment might lead to the difference in the free energy [26], thus leading to increased ΔE_p. In Fig. 4d, on L-Cys/L-CCNT-3/GCE, the ΔE_p of Tyr enantiomers increases to 24 mV with the E_p of L-Tyr and D-Tyr at 0.908 V (curve g) and 0.884 V (curve h). The greater ΔE_p of Tyr enantiomers shows that L-CCNT-3 and L-Cys have a synergistic reaction on the discriminate of L-Tyr and D-Tyr. The enantiopure chiral structure of L-CCNT-3 and steric interaction of L-Cys/L-CCNT-3 with the enantiomers lead to the higher E_p of L-Tyr and lower E_p of D-Tyr. The increased current of D-Tyr than L-Tyr on L-Cys/L-CCNT-3/GCE also agrees with the potential signal of enantiomers. These data indicate that the L-Cys/L-CCNT-3 interface shows excellent chiral recognition performance based on peak potential and peak current signals.

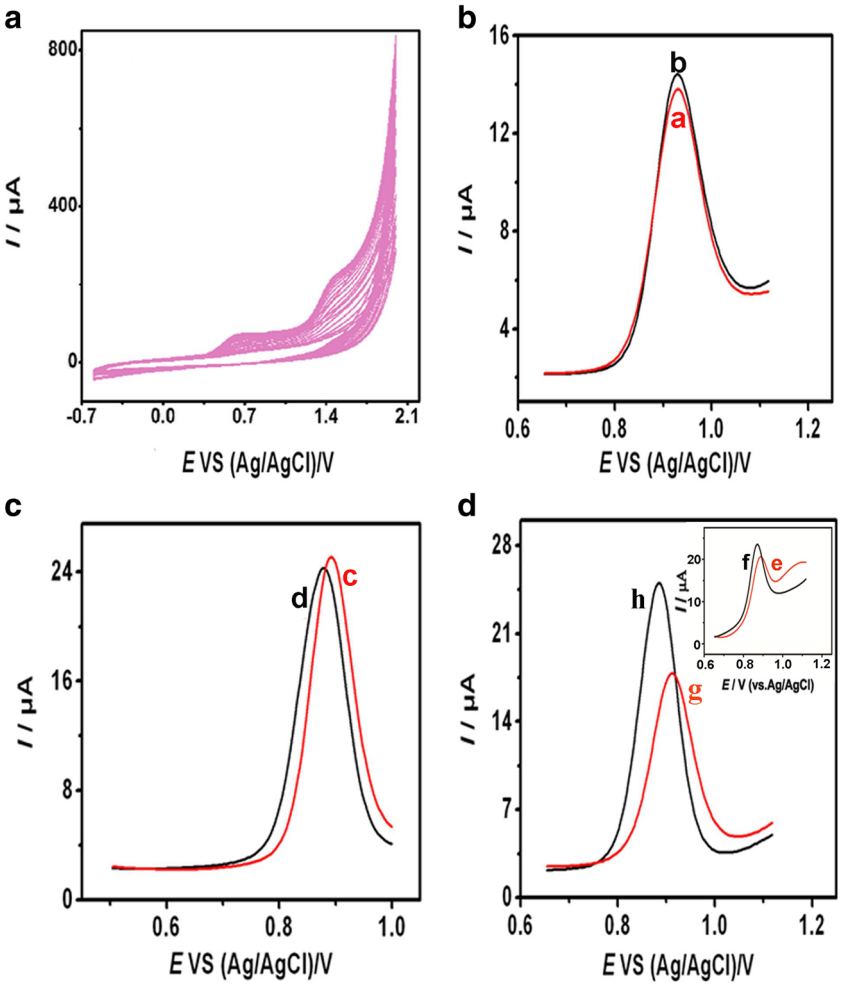

Fig. 4 **a** CVs modify 0.01 M L-Cys on GCE, scan rate: 100 mV/s. **b** Different potential voltammograms (DPVs) of **a** L-Tyr and **b** D-Tyr on GCE. **c** DPVs of **c** L-Tyr and **d** D-Tyr on L-Cys/GCE. **d** Inset: DPVs of **e** L-Tyr and **f** D-Tyr on L-CCNT-3/GCE. DPVs of **g** L-Tyr and **h** D-Tyr on L-Cys/L-CCNT-3/GCE. L-Tyr and D-Tyr concentration: 0.75 mM

Optimization of experimental condition

Option of chiral carbon nanotubes

Chiral carbon nanotubes are the key nanomaterial in this experiment. Three kinds of L-CCNTs (L-CCNT-1, L-CCNT-2, and L-CCNT-3) carbonized at 500, 700, and 900 °C were used as the chiral catalysts in the Tyr recognition experiments.

As is shown in Fig. 5a, L-Cys/L-CCNT-1/GCE shows peak potential of 0.910 V (line a) and 0.898 V (line b) for L-Tyr and D-Tyr, and the ΔE_p is 12 mV. While L-Cys/L-CCNT-2/GCE (Fig. 5b) and L-Cys/L-CCNT-3/GCE (Fig. 5c) show the ΔE_p of 16 mV (lines c and d) and 24 mV (lines e and f), these data suggest that L-CCNT-3 has better chiral recognition ability than L-CCNT-1 and L-CCNT-2. Therefore, L-CCNT-3 with largest ΔE_p for Tyr enantiomers is selected as the optimum material in the next experiments.

Optimization of sweep cycle of L-Cys

Sweep cycle plays an important role in modifying the electrode with L-Cys. The modification condition is investigated by varying sweep cycles of L-Cys from 5 to 30 on different electrodes (Fig. 5d). It can be clearly seen that the ΔEp of Tyr enantiomers on L-Cys/L-CCNT-1/GCE keeps stable when the sweep cycles increase. While ΔEp of Tyr enantiomers on L-Cys/L-CCNT-2/GCE and L-Cys/L-CCNT-3/GCE first increase with sweep cycle and then decrease, the L-Cys/L-CCNT-3/GCE with the sweep cycles of 15 shows the most distinct ΔEp for L-Tyr and D-Tyr. This may be attributed to the saturation of enantioselective reaction sites of adsorbed CyA on electrode. According to above results, 15 cycle and L-CCNT-3 are chosen as the detection condition in the following experiments.

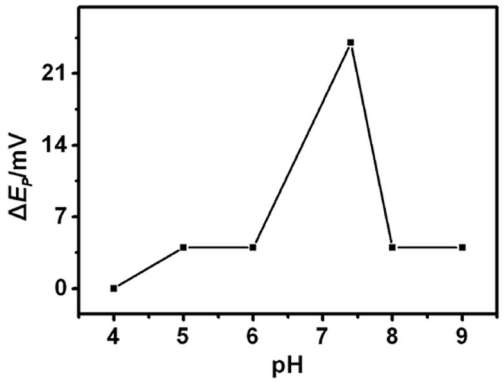

Fig. 6 The relationship between ΔEp of L/D-Tyr and pH. Concentration of L-Tyr and D-Tyr: 0.75 mM

Optimization of pH

The electrooxidation of 0.75 mM L-Tyr and D-Tyr on L-Cys/L-CCNT-3/GCE at different pH values in 0.1 M PBS was researched. As can be seen from the plot of (ΔE_P)-pH (Fig. 6), the ΔE_P of L-Tyr and D-Tyr increases from pH 4.0 and reaches top value at pH 7.4, then the ΔE_P decreases sharply. The reason

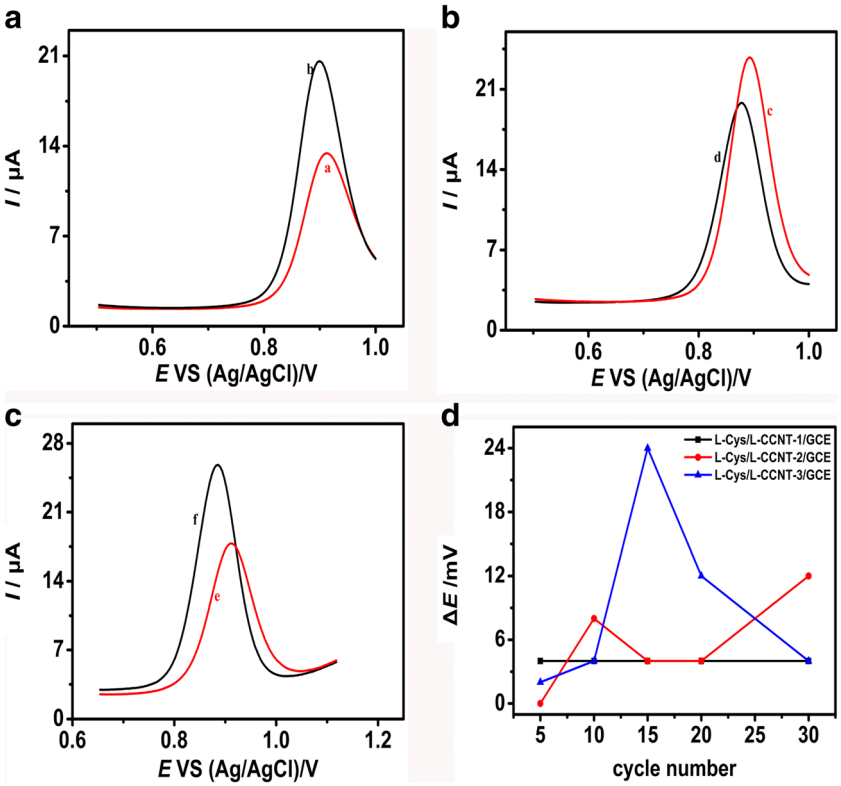

Fig. 5 **a** DPVs of **a** L-Tyr on L-Cys/L-CCNT-1/GCE, **b** D-Tyr on L-Cys/L-CCNT-1/GCE. **b** DPVs of **c** L-Tyr on L-Cys/L-CCNT-2/GCE, **d** D-Tyr on L-Cys/L-CCNT-2/GCE. **c** DPVs of **e** L-Tyr on L-Cys/L-CCNT-3/GCE and **f** D-Tyr on L-Cys/L-CCNT-3/GCE. L-Tyr and D-Tyr concentration: 0.75 mM; pulse amplitude: 0.05 V, pulse width: 0.05 s, pulse period: 0.5 s. **d** The different ΔEp of L-Tyr and D-Tyr on L-Cys/L-CCNT-1/GCE, L-Cys/L-CCNT-2/GCE, and L-Cys/L-CCNT-3/GCE with different Cys sweep cycles

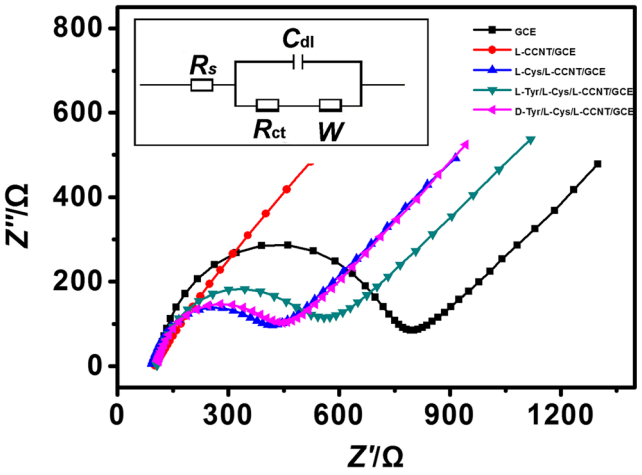

Fig. 7 Nyquist plots at GCE, L-CCNT-3/GCE, L-Cys/L-CCNT-3/GCE, L-Tyr/L-Cys/L-CCNT-3/GCE, and D-Tyr/L-Cys/L-CCNT-3/GCE in 5 mM $Fe(CN)_6^{3-/4-}$ (1:1) containing 0.1 M KCl within a frequency range from 1.0 to 10 kHz. The measurements were operated at open circuit potential

is that the pH of phosphate buffer solution plays an important role in enantiospecificity of amino acid [16, 27, 28]. Under near neutral pH, Tyr and CyA are zwitterions; the electrostatic repulsion is weak, which allows favorable interaction for chiral recognition [29, 30]. That is to say, under near neutral pH, the interaction of L-CyA with D-Tyr is more stronger than that under other pH, while the space mismatching of L-CyA with L-Tyr still exists, thus leading to increased difference of potential for L-Tyr and D-Tyr under near neutral pH (pH 7.4). Therefore, pH 7.4 is selected for the determination of L-Tyr and D-Tyr.

Electrochemical impedance spectroscopy research

It is well known that EIS technique is a powerful method to characterize the electrochemical processes occurring at the solution/electrode interface. In order to research the interactions of L-Tyr or D-Tyr with our prepared chiral electrode interface, EIS was employed in 5.0 mM $K_3Fe(CN)_6$–$K_4Fe(CN)_6$ and 0.1 M KCl solution at open potential. The curve of EIS includes a semicircle portion and a linear portion, with the former at higher frequencies corresponding to the electron-transfer limited process and the latter at lower frequencies to the diffusion process. The surface electron-transfer resistance (*R*ct) equals to the diameter of the semicircle, which can be used to describe the interface properties of the electrode. Randles equivalent circuit model (inset of Fig. 7) was used to fit the obtained impedance data (where *R*s represents the Warburg impedence, C_{dl}, double layer capacitance, *W*, resulting from the diffusion of ions from the bulk electrolyte to the electrode interface, and *R*ct the electron-transfer resistance). From the impedance spectra, the *R*ct of L-CCNT/GCE (28 Ω) reduced enormously as compared with that of GCE (659 Ω). This indicates that the L-CCNTs greatly facilitate the electron transfer of the electrode. While for L-Cys/L-CCNT/GCE, the *R*ct is increased to 308 Ω, indicating the successful polymerization of L-Cys on L-CCNT/GCE. The *R*ct (323 Ω) slightly increases after immersing L-Cys/L-CCNT/GCE in D-Tyr, which could be understood by the spatial interaction of L-Cys/L-CCNT with D-Tyr. The *R*ct (426) is further dramatically increased after L-Tyr is anchored onto the surface of L-Cys/L-CCNT/GCE. The greatly increased *R*ct of L-Tyr/L-Cys/L-CCNT/GCE suggests that L-Tyr has larger steric hindrance with L-Cys/L-CCNT/GCE than D-Tyr. The result agrees well with the changes of potential signals for L-Tyr and D-Tyr in DPVs.

Table 1 Determination of L-tyrosine in L-tyrosine tablet sample

Sample	Labeled (mg/mL)[a]	Added (mg/mL)	Found (mg/mL)	Recovery (%)
1	0.0650	0.0065	0.0718	104.6
2	0.0650	0.0130	0.0781	100.8
3	0.0650	0.0195	0.0852	103.6

[a] The sample was diluted 20 times with pH 7.4 PBS

Application of Tyr chiral recognition in their racemic solution

According to the above optimized experimental conditions, our prepared L-Cys/L-CCNT-3/GCE may realize electrochemical chiral detection of L-Tyr and D-Tyr in racemic solution based

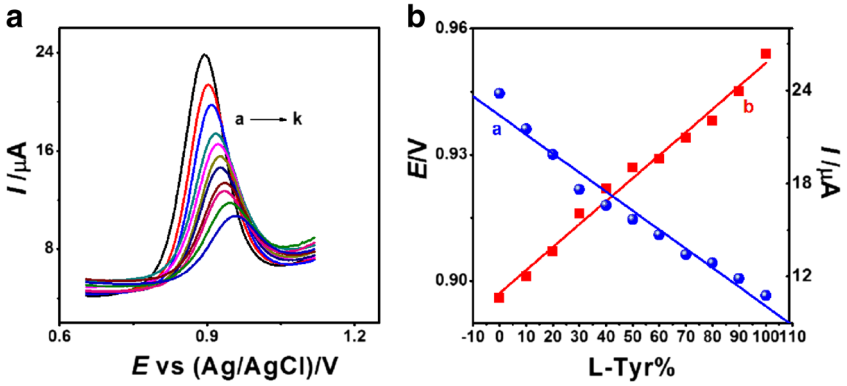

Fig. 8 **a** DPVs of different L-Tyr% of 0.75 mM Tyr racemic mixture on L-Cys/L-CCNT-3/GCE. L-Tyr percentage (a to k, %): 0, 10, 20, 30, 40, 50, 60, 70, 80, 90, 100. **b** Relationship between **a** *I*p (blue line), **b** *E*p (*red line*) and different L-Tyr%

on the potential difference signals. Figure 8a shows the DPVs of different L-Tyr% (a-k: 0, 10, 20, 30, 40, 50, 60, 70, 80, 90, 100) of 0.75 mM Tyr racemic mixture on L-Cys/L-CCNT-3/GCE. It can be clearly seen that the peak potential positive shift and the peak current decrease with the increased L-Tyr%. Figure 8b exhibits the good linear relationship of L-Tyr% with peak potential and current. The detection limit, based on a signal-to-noise ratio of 3, was calculated to be 2.93 μM for L-Tyr. The result shows that L-Cys/L-CCNT-3/GCE can quantitatively detect L-Tyr and D-Tyr enantiomers in their racemic solution based on potential and current signals simultaneously. According to Dalgliesh's theory [31] and "three-point attachment model," an interaction in at least three configuration-dependent points is needed for a chiral selector to recognize entantiomers [32]. Thermodynamic enantioselectivity arises from the difference in the intensity of the interaction, i.e., the difference in the stability of two possible diastereomeric adducts formed in the course of the interaction. Chiral discrimination of the enantiomers can be based on the thermodynamic enantioselectivity and the difference in the free energy [32]. In this study, the chiral structure of L-CCNT, the aromatic ring of Tyr, and the intermolecular hydrogen bond between CyA and Tyr could possibly give this "three-point" attachment. The difference of L-Cys/L-CCNT/GCE and L/D-Tyr attachment might lead to the difference in the free energy, which reflects as potential shift in electrochemical measurements [26]. Because of the space structure of L-Cys/L-CCNT, it may have stronger attachment with D-Tyr than L-Tyr, leading to lower free energy; therefore, the potential decreases and current increases with the increased (decreased) of D-Tyr% (L-Tyr%).

Determination of L-tyrosine in pharmaceutical formulations

For the purpose of proving its practical application, the prepared electrode was used to determine the L-tyrosine tablet. L-tyrosine sample was prepared by dissolving a L-tyrosine caplet (containing 500 mg of L-tyrosine) into 384-mL formic acid solution (1:1). The determination was realized by the standard addition method, and the results are listed in Table 1. It was found that the recoveries of the proposed method were satisfactory (100.8 ~ 104.6%).

Conclusions

In this work, a kind of novel left-handed chiral carbonaceous nanotubes were prepared and used as the chiral electrocatalyst for Tyr enantiomer recognition. The electrochemical determination of L- and D-tyrosine in their mixed solution was successfully achieved based on different oxidation potential signals on L-Cys/L-CCNT-3/GCE. What is more, the peak potential and peak current linear variation with the increased percentage of L-Tyr in racemic mixture. This work builds a novel potential type electrochemical chiral biosensing system based on chiral carbonaceous nanotubes; moreover, it realizes the distinguished and quantitative determination of Tyr enantiomers with satisfactory results. This work is of great importance in real chiral biosensing research.

Acknowledgements The authors gratefully acknowledge the support from the National Natural Science Foundation of China (No. 21505031), colleges and universities science technology research project of Hebei Province (No. Z2015096) and the Natural Science Foundation of Hebei Province (No. B2016201018).

References

1. Berthier D, Buffeteau T, Léger J, Oda R, Huc I (2002) From chiral counterions to twisted membranes. J Am Chem Soc 122:13486–13494
2. Schröder T, Schmitz K, Niemeier N, Balaban TS, Krug HF, Schepers U, Bräse S (2007) Solid-phase synthesis, bioconjugation, and toxicology of novel cationic oligopeptoids for cellular drug delivery. Bioconjug Chem 18:342–354
3. Uray G, Maier NM, Niederreiter KS, Spitaler MM (1998) Diphenylethanediamine derivatives as chiral selectors: VIII. Influence of the second amido function on the high-performance liquid chromatographic enantioseparation characteristics of (N-3,5-dinitrobenzoyl)-diphenylethanediamine based chiral stationary phases. J Chromatogr A 799:67–81
4. Li M, Liu X, Jiang F, Guo LP, Yang L (2011) Enantioselective open-tubular capillary electrochromatography using cyclodextrin-modified gold nanoparticles as stationary phase. J Chromatogr A 1218:3725–3729
5. Guo HS, Kim JM, Chang SM, Kim WS (2009) Chiral recognition of mandelic acid by l-phenylalanine-modified sensor using quartz crystal microbalance. Biosens Bioelectron 24:2931–2934
6. Su WC, Zhang WG, Zhang S, Fan J, Yin X, Luo ML, Ng SC (2009) A novel strategy for rapid real-time chiral discrimination of enantiomers using serum albumin functionalized QCM biosensor. Biosens Bioelectron 25:488–492
7. Liang H, Ling T, Rick JF, Chou T (2005) Molecularly imprinted electrochemical sensor able to enantroselectivly recognize d and l-tyrosine. Anal Chim Acta 542:83–89
8. Bustos E, García JE, Bandala Y, Godínez LA, Juaristi E (2009) Enantioselective recognition of alanine in solution with modified gold electrodes using chiral PAMAM dendrimers G4.0. Talanta 78:1352–1358
9. Pandey I, Kant R (2016) Electrochemical impedance based chiral analysis of anti-ascorbutic drug: l-ascorbic acid and d-ascorbic acid using C-dots decorated conductive polymer nano-composite electrode. Biosens Bioelectron 77:715–724
10. Guo DM, Huang YH, Chen C, Chen Y, Fu YZ (2014) A sensing interface for recognition of tryptophan enantiomers based on porous cluster-like nanocomposite films. New J Chem 38:5880–5885
11. Guo LJ, Zhang Q, Huang YH, Han Q, Wang YH, Fu YZ (2013) The application of thionine–graphene nanocomposite in chiral sensing for tryptophan enantiomers. Bioelectrochemistry 94:87–93
12. Yu LY, Liu Q, Wu XW, Jiang XY, Yu JG, Chen XQ (2015) Chiral electrochemical recognition of tryptophan enantiomers at a multi-walled carbon nanotube–chitosan composite modified glassy carbon electrode. RSC Adv 5:98020–98025
13. Ou J, Zhu YH, Kong Y, Ma JF (2015) Graphene quantum dots/β-cyclodextrin nanocomposites: a novel electrochemical chiral

interface for tryptophan isomer recognition. Electrochem Commun 60:60–63
14. Gu XG, Tao YX, Pan Y, Deng LH, Bao LP, Kong Y (2015) DNA-inspired electrochemical recognition of tryptophan isomers by electrodeposited chitosan and sulfonated chitosan. Anal Chem 87: 9481–9486
15. Kimmel DW, LeBlanc G, Meschievitz ME, Cliffel DE (2012) Electrochemical sensors and biosensors. Anal Chem 84:685–707
16. Wang Y, Yin X, Shi M, Li W, Zhang L, Kong J (2006) Probing chiral amino acids at sub-picomolar level based on bovine serum albumin enantioselective films coupled with silver-enhanced gold nanoparticles. Talanta 69:1240–1245
17. Li XL, Tu XM, Zaric S, Welsher K, Seo WS, Zhao W, Dai HJ (2007) Selective synthesis combined with chemical separation of single-walled carbon nanotubes for chirality selection. J Am Chem Soc 129:15770–15771
18. Chen Y, Wei L, Wang B, Lim S, Ciuparu D, Zheng M, Chen J, Zoican C, Yang YH, Haller GL, Pfefferle LD (2007) Low-Defect, purified, narrowly (*n*,*m*)-dispersed single-walled carbon nanotubes grown from cobalt-incorporated MCM-41. ACS Nano 1:327–336
19. Yu YT, Qiu HB, Wu XW, Li HC, Li YS, Sakamoto Y, Inoue Y, Sakamoto K, Terasaki O, Che SA (2008) Synthesis and characterization of silica nanotubes with radially oriented mesopores. Adv Funct Mater 18:541–550
20. Liu SH, Duan YY, Feng XJ, Yang J, Che SA (2013) Synthesis of enantiopure carbonaceous nanotubes with optical activit. Angew Chem Int Ed 52:6858–6862
21. Yang SB, Feng XL, Wang XC, Müllen K (2011) Graphene-based carbon nitride nanosheets as efficient metal-free electrocatalysts for oxygen reduction reactions. Angew Chem Int Ed 50:5339–5343
22. Wang CY, Wang ZX, Guan J, Hu XY (2006) Voltammetric determination of meloxicam in pharmaceutical formulation and human serum at glassy carbon electrode modified by Cysteic acid formed by electrochemical oxidation of L-cysteine. Sensors 6:1139–1152
23. Brunetti B, Desimoni E (2009) Determination of theophylline at a cysteic acid modified glassy carbon electrode. Electroanalysis 21: 772–778
24. Fei S, Chen J, Yao S, Deng G, He D, Kuang Y (2005) Electrochemical behavior of L-cysteine and its detection at carbon nanotube electrode modified with platinum. Anal Biochem 339: 29–35
25. Spãtaru N, Sarada BV, Popa E, Tryk DA, Fujishima A (2001) Voltammetric determination of L-cysteine at conductive diamond electrodes. Anal Chem 73:514–519
26. Scholz F, Gulaboski R (2005) Gibbs energies of transfer of chiral anions across the interface water|chiral organic solvent determined with the help of three-phase electrodes. Faraday Discuss 129:169–177
27. Chen Q, Zhou J, Han Q, Wang YH, Fu YZ (2012) Electrochemical enantioselective recognition of tryptophane enantiomers based on chiral ligand exchange. Colloids Surf, B 92:130–135
28. Sulaiman Y, Kataky R (2012) Chiral acid selectivity displayed by PEDOT electropolymerised in the presence of chiral molecules. Analyst 137:2386–2393
29. Shamsi SA, Valle BC, Billiot F, Warner IM (2003) Polysodium n-undecanoyl-L-leucylvalinate: a versatile chiral selector for micellar electrokinetic chromatography. Anal Chem 75:379–387
30. Agnew-Heard KA, Sánchez Peña M, Shamsi SA, Warner IM (1997) Studies of polymerized sodium n-undecylenyl-L-valinate in chiral micellar electrokinetic capillary chromatography of neutral, acidic, and basic compounds. Anal Chem 69:958–964
31. Dalgliesh CE (1952) The optical resolution of aromatic amino-acids on paper chromatograms. J Chem Soc 3940-3942
32. Davankov VA (1997) The nature of chiral recognition: is it a three-point interaction. Chirality 9:99–102